

# Bubble walls in the holographic D3/probe D7 system with magnetic field

**Wanxiang Fan**

Supervised by Nick Evans

School of Physics and Astronomy,  
University of Southampton

13/11/2024

Based on Nick Evans, W. Fan, arXiv:2408.10835



University of  
**Southampton**

14/12/2024

# Outline

---

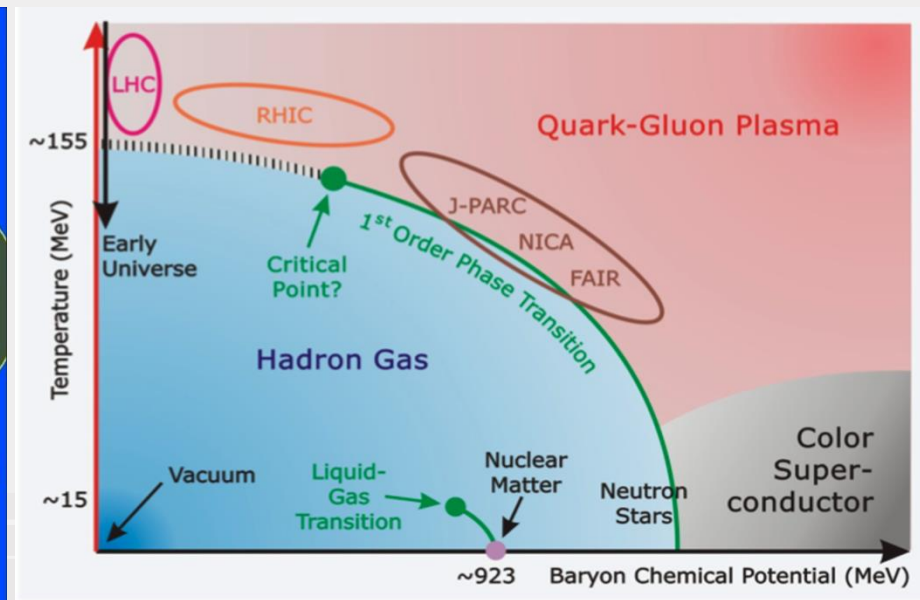
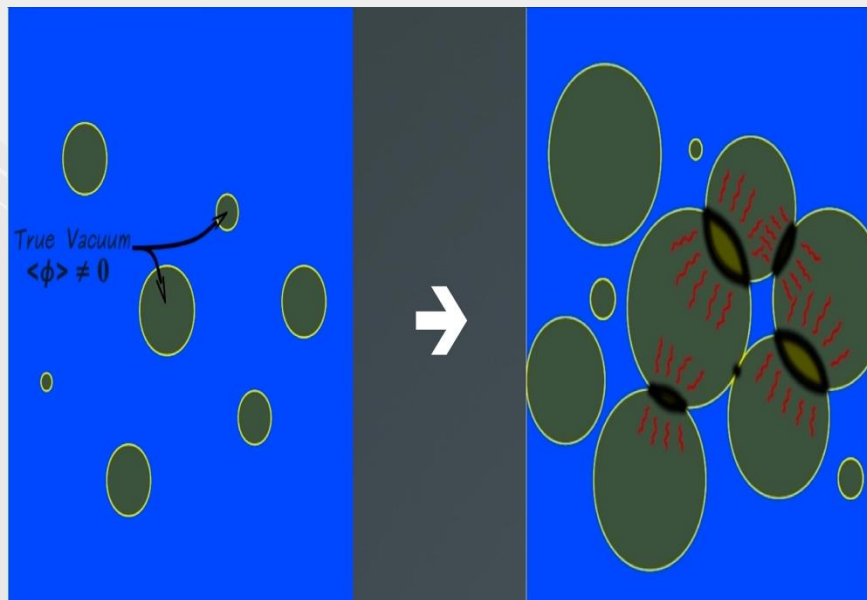
- **Motivations**
- We will talk about **D3/D7 model** which dual so called Weyl semimetal system. Such system shows **first order phase transition** ending with critical point in the **M-B Plane** (Mass, Magnetic Field, Temperature).
- The Dial-able Bubble Wall Motion at **zero/finte temperature** is calculated with proper boundary conditions.
- We develop a method to simulate the bubble wall motion at **finite temperature** with few examples to be presented.



# Motivation and background

## Why a holographic model to compute the bubble wall velocity?

- ❑ A **first order phase transition** in the early Universe would generate the formation of bubbles. The growth and collision of bubbles may generate **gravitational wave signals**, which is of interest in this phenomena for the current and future gravitational wave detectors.
- ❑ A key parameter for simulating the gravitational wave phenomena is **the speed of the bubble wall**, which is difficult to predict even for perturbative theory.
- ❑ If the system undergoing the phase transition were to be **strongly coupled** (in the spirit of the QCD phase transition) then calculation becomes yet harder. It is worth to try the calculation in a **holographic model**.



# Motivation and background

## Holographic Tools: AdS/CFT correspondence

Maldacena: 9711200

Witten: 9802150

Gubser, Klebanov, Polyakov: 9802109

Quantum field theory  
in  $d$  dimensions

$\mathcal{N} = 4$  Super Yang-Mills  
With gauge group  $SU(N)$   
with parameters  $g_{ym}$  and  
 $N$

$AdS/CFT$

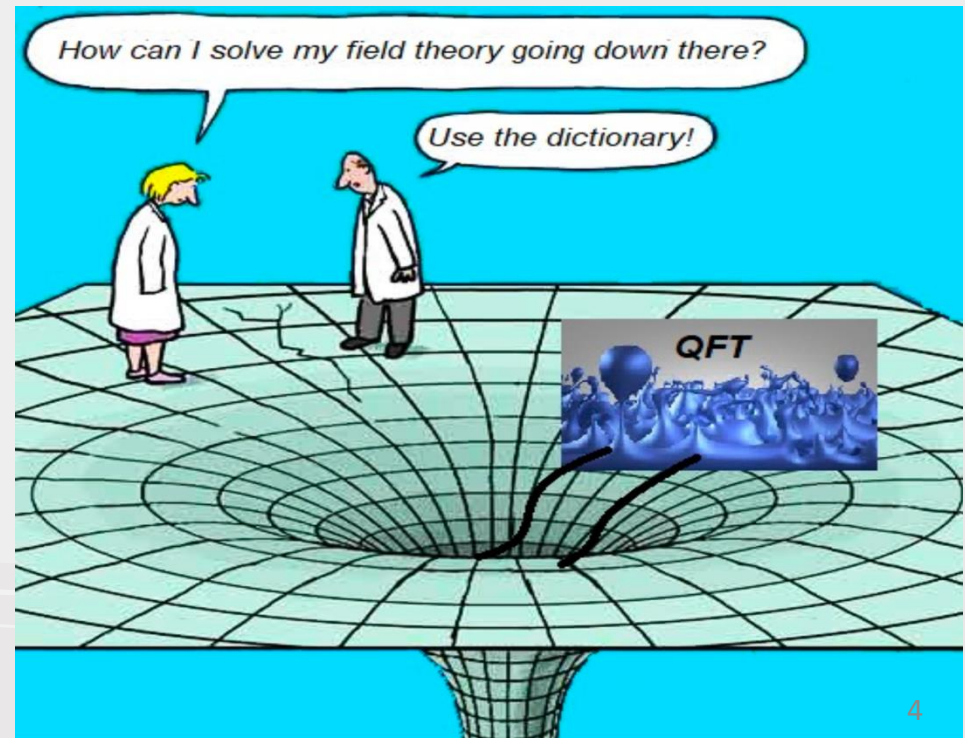
Holography

String theory in  $(d+1)$ -dim  
Anti-de Sitter ( $AdS_5$ )

Type IIB String theory on  
asymptotically  $AdS_5 \times S^5$   
with parameters  $g_s$  and  
 $L/\sqrt{\alpha'}$

$$g_{ym}^2 = 2\pi g_s$$
$$2 g_{ym}^2 N = \frac{L^4}{\alpha'^2}$$

- In large  $N$  and large  $\lambda = g_{ym}^2 N$  limit, strongly coupled field theory is equivalent to weakly coupled gravity.
- Hence, we can use this tool to calculate the observables (condensate, two-point function...) of the strongly coupled system using classical gravity techniques.

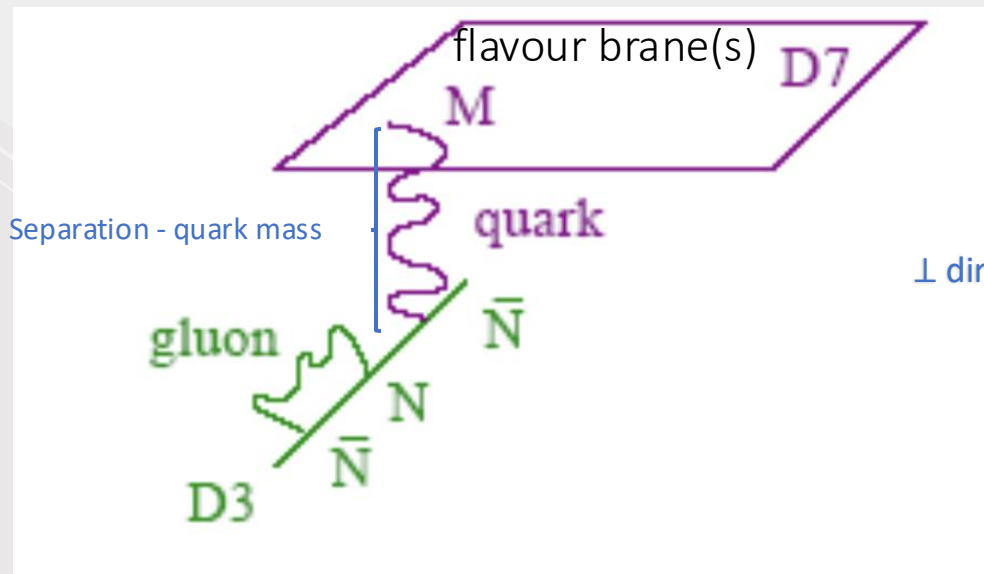


# Motivation and background

Andreas Karch, Emanuel Katz : 0205236

## AdS/CFT correspondence with probe branes: D3/probe D7

- ❑ The original AdS/CFT (large  $N$  D3 branes) has gauge field (e.g. gluons in QCD) only.
- ❑ To study the strongly coupled system with matter field (e.g. quarks in QCD), embed probe D7 branes in the background geometry (back reaction is not considered in the probe limit).
- ❑ Conceptually, open string on the D7 branes (7-7 string) is interpreted as meson.
- ❑ Open string on D3 branes (3-3) are interpreted as gluon;
- ❑ Open string connecting D3 and D7 branes (3-7/7-3 string) which is interpreted as quark/antiquark.



world volume coordinates

Holographic radius (energy scale in the picture of RG flow)

	t	x	y	z	r	$\beta_1$	$\beta_2$	$\beta_3$	R	$\phi$
D3	x	x	x	x						
D7	x	x	x	x	x	x	x	x		

world volume coordinates

⊥ direction

# Motivation and background

## D3/probe D7

DBI action of D7 branes:

The volume of D7

$$S_{D7} = -N_f T_{D7} \int d^8 \xi \sqrt{-\det(P[G] + F)}$$

	world volume coordinates				Holographic radius					
	t	x	y	z	r	$\beta_1$	$\beta_2$	$\beta_3$	R	$\phi$
D3	x	x	x	x						
D7	x	x	x	x	x	x	x	x		

world volume index      target space index

- P[G] is the pullback of the metric on D7 brane. i.e.  $G_{ab} = G_{MN} \partial_a X^M \partial_b X^N$
- F is field strength of the gauge field A living on the D7 branes, in components

$$F = F_{\mu\nu} dx^\mu \wedge dx^\nu = \frac{1}{2} (\partial_\mu A_\nu - \partial_\nu A_\mu) dx^\mu \wedge dx^\nu$$

- The D7 branes are embedded in the  $AdS_5 - Schwarzschild$  geometry with finite temperature:

$$ds^2 = \frac{\rho^2}{L^2} \left( -\frac{g^2(\rho)}{h(\rho)} dt^2 + h(\rho)(dx^2 + dy^2 + dz^2) \right) + \frac{L^2}{\rho^2} (dr^2 + r^2 ds_{S^3}^2 + dR^2 + R^2 d\phi^2)$$

$$\rho^2 = r^2 + R^2, \quad g(\rho) = 1 - \frac{\rho_H^4}{\rho^4}, \quad h(\rho) = 1 + \frac{\rho_H^4}{\rho^4}$$

L: radius of  $AdS_5$  and  $S^5$ . (in practice  $L = 1$ )

$\rho_H$ : the radius of the black hole.

# Motivation and background

## The Weyl Semimetal Model

Kazem Fadafan, Andy O'Bannon, etc : 2012.11434

- Weyl and Dirac semi-metals are materials in which an insulator, when in the presence of some background field, develops light degrees of freedom that conduct strongly.
- The simplest model is a massive fermion which couples to an axial gauge field  $A_j^5$ :

$$\mathcal{L} = \bar{\psi}(i\gamma^\mu \partial_\mu - m + A_j^5 \gamma^j \gamma^5)\psi$$

- When the axial gauge field develops a vev, (e.g. in z direction  $A_z^5 = b/2$ ), the eigenenergies of the system are

$$E^2 = k_x^2 + k_y^2 + \left( \frac{b}{2} \pm \sqrt{k_z^2 + m^2} \right)^2$$

- There are two Weyl spinor, i.e. the zero eigenenergy with corresponding momentum  $(k_x, k_y, k_z) = (0, 0, \pm \sqrt{(\frac{b}{2})^2 - m^2})$ , which can now be excited.

## The holographic dual of Weyl Semimetal Model: D3/probe D7

The ansatz for the D7 embedding:

- $R = R(r)$
- $\phi(z) = b z$  – corresponding to the axial gauge field coupling
- Background Magnetic field  $B_x = F_{yz}$  which is perpendicular to direction of  $b$ .

	world volume coordinates					Holographic radius				
	t	x	y	z	r	$\beta_1$	$\beta_2$	$\beta_3$	R	$\phi$
D3	x	x	x	x						
D7	x	x	x	x	x	x	x	x		

The Lagrangian density is given by

$$\mathcal{L}_{D7} = -r^3 gh \sqrt{\left(1 + \frac{L^4 B_x^2}{h^2(r^2 + R^2)^2} + \frac{L^4 b^2 R^2}{h(r^2 + R^2)^2}\right) (1 + R'^2)}$$

$$\longrightarrow R(r) = M + \frac{\langle \bar{q} q \rangle}{r^2} + \dots$$

There are three classes of embeddings (BCs):

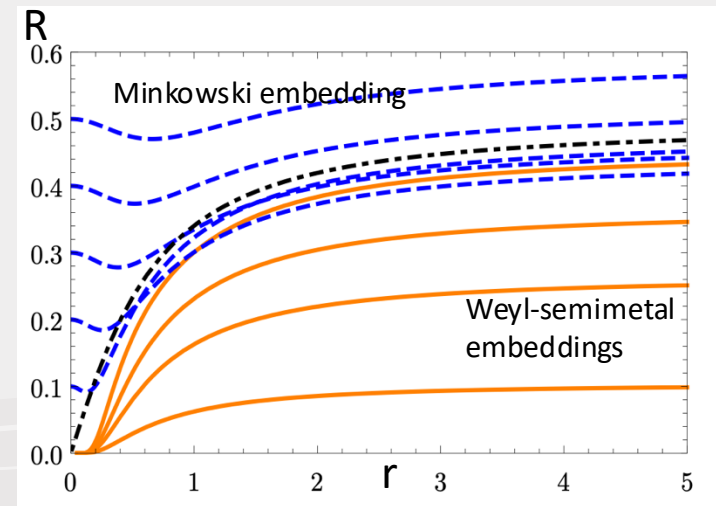
- Minkowski embeddings:  $R(0) = m_{ir} \neq 0, R'(0) = 0$
- Critical embeddings: approaches  $R_0 = 0$  linearly in  $r$ :

$$R_c(r) = \frac{r}{\sqrt{3}} - \frac{32r^3}{27\sqrt{3}L^4b^2} + \mathcal{O}(r^5)$$

- Weyl-semimetal embeddings:  $R(r)$  vanishes exponentially quickly as  $r \rightarrow 0$

$$R(r) = \eta \frac{e^{-L^2b/r}}{\sqrt{r}} [1 + \mathcal{O}(r^2)]$$

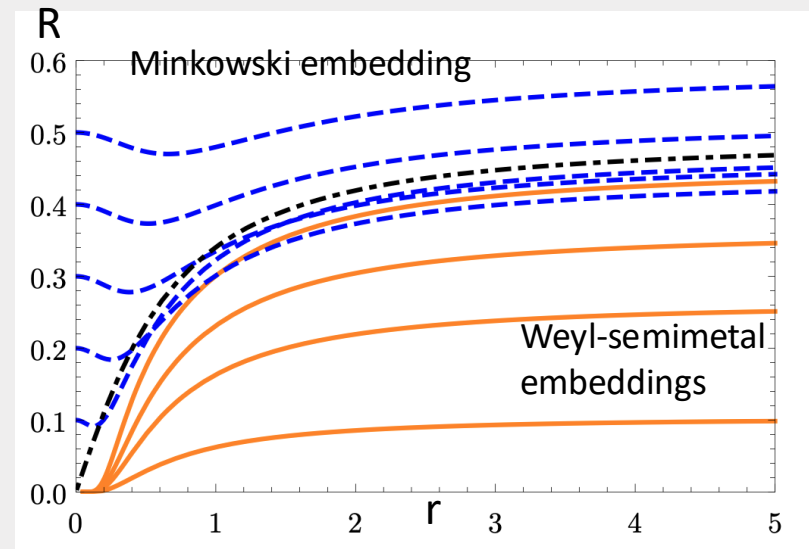
- If the magnetic background field  $B$  switch on, only Minkowski embedding survives (see in next slide).



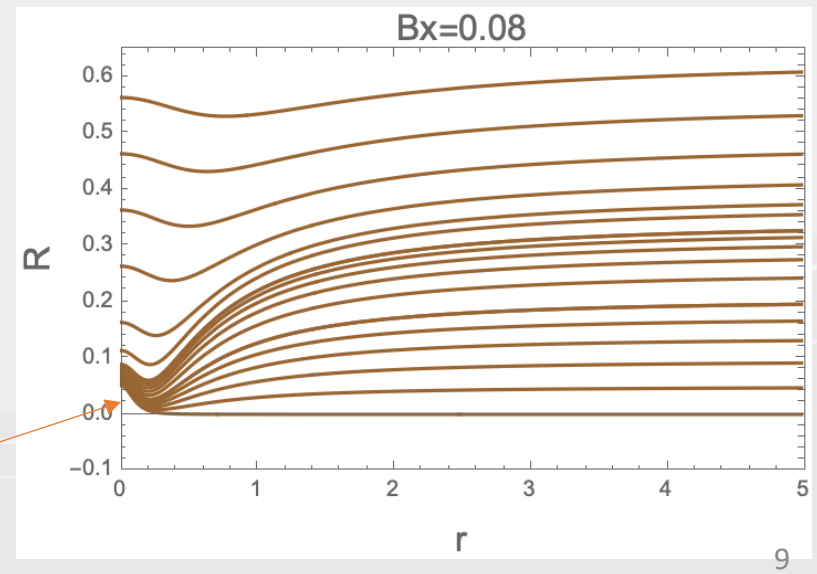
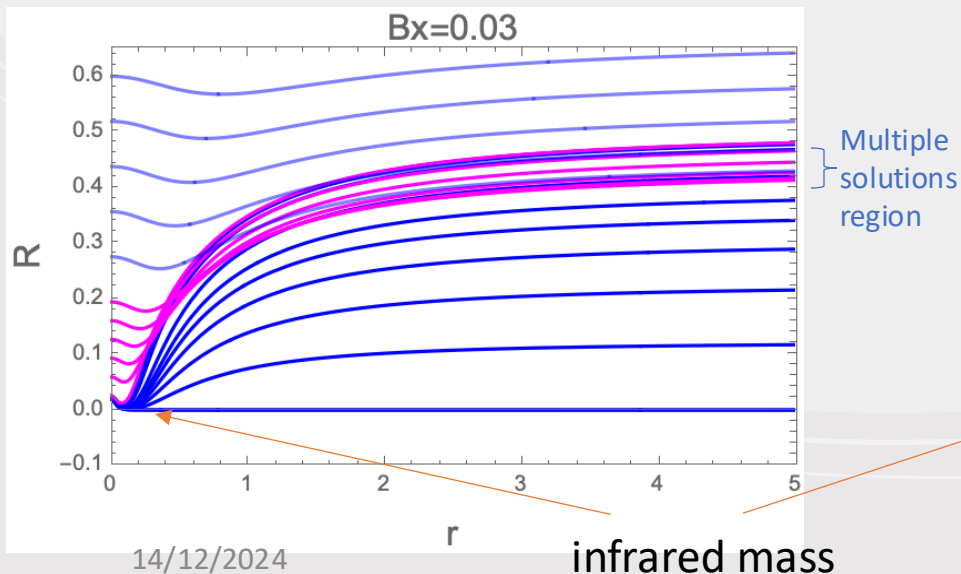
# I. Phase Transition:

## Embeddings with different IR mass at zero temperature

- ❑ In the presence of  $B$ , there is always an **infrared mass** generated.
- ❑ There is a **first order phase transition** for small  $B$ . (Multiple solutions with a region of UV mass)
- ❑ The first order phase transition region shrinks and finally disappears as  $B$  increases.



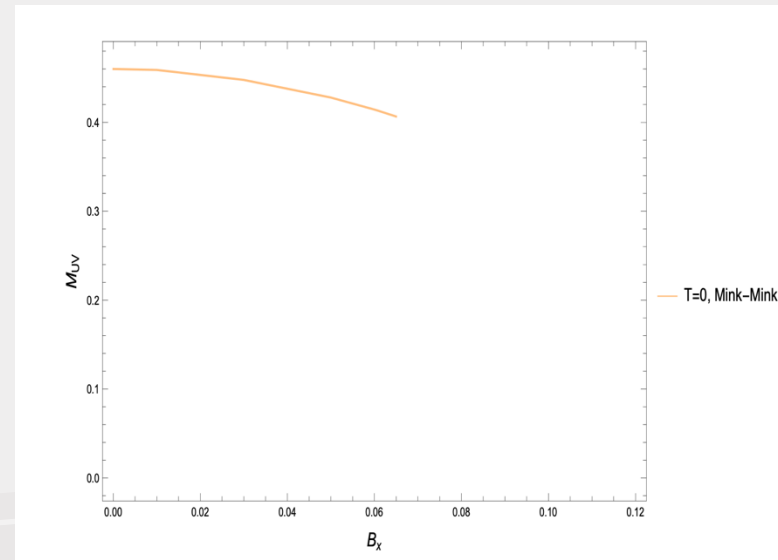
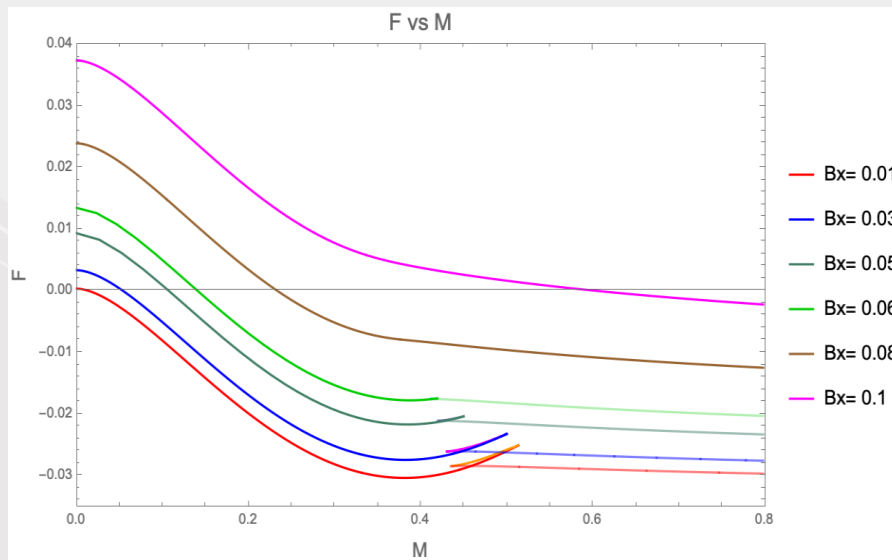
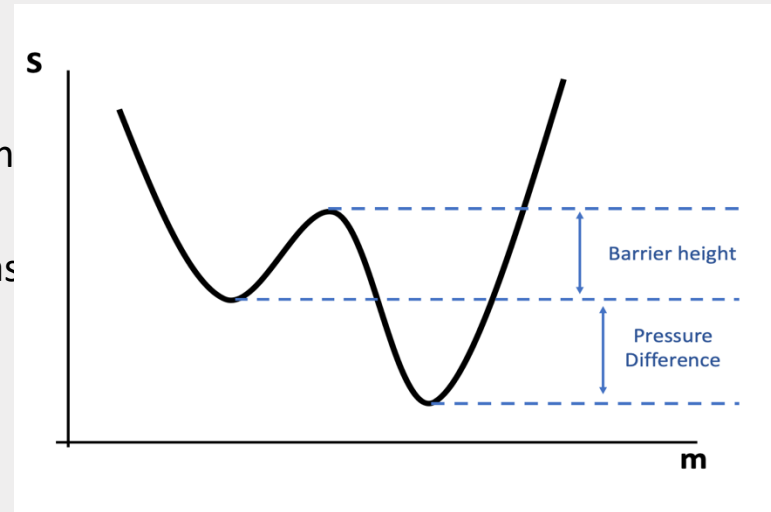
Switch on the background  $B$  field



# I. Phase Transition

## The Free Energy

- ❑ The swallow tail structure  $\Rightarrow$  First order phase transition
- ❑ The swallow structure  $\Rightarrow$  Critical point in the B-M plane as shown in the phase diagram
- ❑ There are three solutions in the swallow tail region for a given UV mass, and we define the parameters: **pressure difference** and **barrier height** as shown on the right.



## II. Bubble Walls

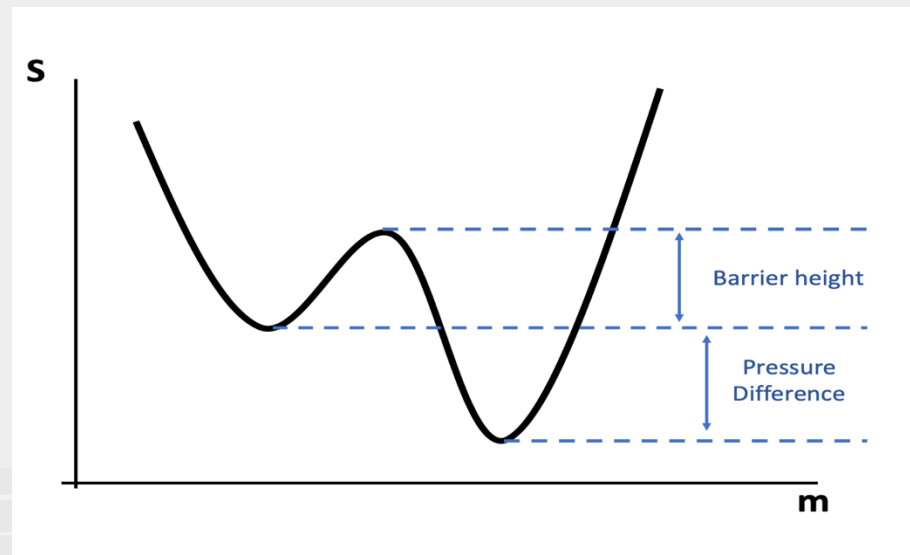
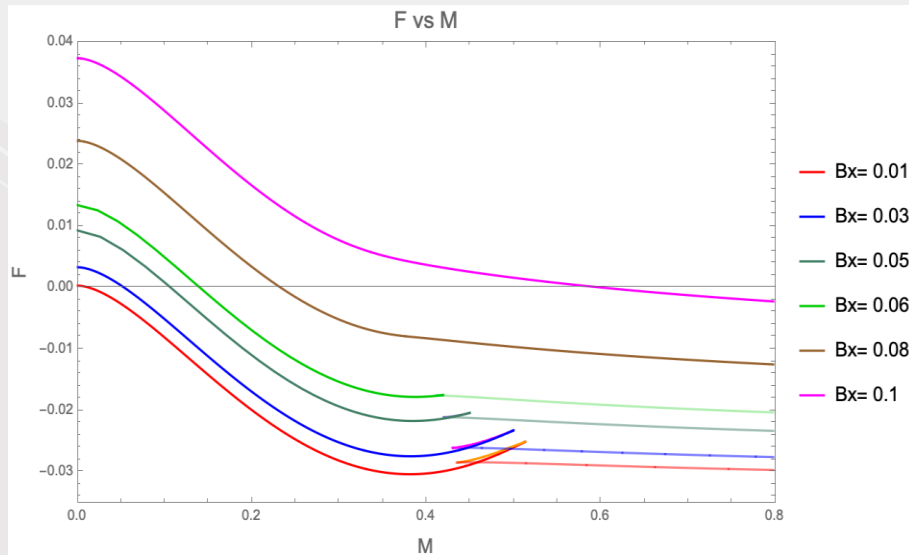
Notation change:

$r \rightarrow \rho$

$R \rightarrow L$

### Parameters of the bubble wall

- ❑ As shown on the left free energy diagram, the theory allow us to control the parameters of the bubble wall in a holographic setting at zero temperature.
- ❑ By moving in the range of mass  $M$  of the swallow tail at fixed  $B$ , we can dial the energy (pressure) differences between the two minima.
- ❑ By increasing magnetic field  $B_x$  we can move along the line of first order transitions towards the critical point.
- ❑ At the critical point, the two local minima converge and the barrier height between them is zero - thus we can dial the barrier height as well.



## II. Bubble Walls

### Dynamics of bubble wall

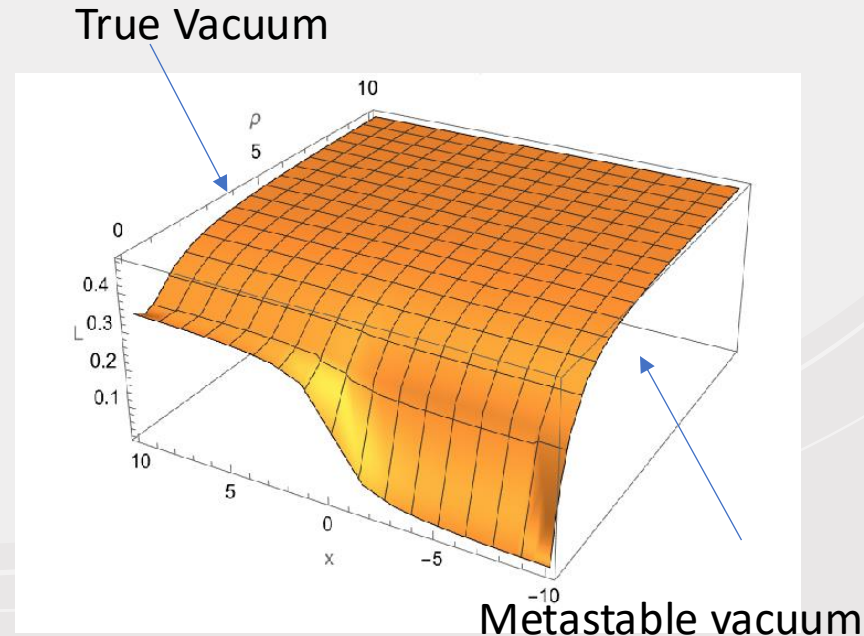
The Lagrangian density for D7 DBI action including variation in the spatial direction  $x$  and time dependence i.e.  $L(\rho, t, x)$

$$\mathcal{L} = \rho^3 gh \sqrt{\left(1 + \frac{B^2}{h^2(\rho^2 + L^2)^2} + \frac{b^2 L^2}{h(\rho^2 + L^2)^2}\right) \left(1 + (\partial_\rho L)^2 + \frac{(\partial_x L)^2}{h(\rho^2 + L^2)^2} - \frac{h}{g^2} \frac{(\partial_t L)^2}{(\rho^2 + L^2)^2}\right)}$$

Where  $g, h$  are the same factor of black hole radius as

Equation of Motion + Initial/Boundary conditions

- Initial conditions:  $L[\rho, 0, x] = L_0[\rho, x]$

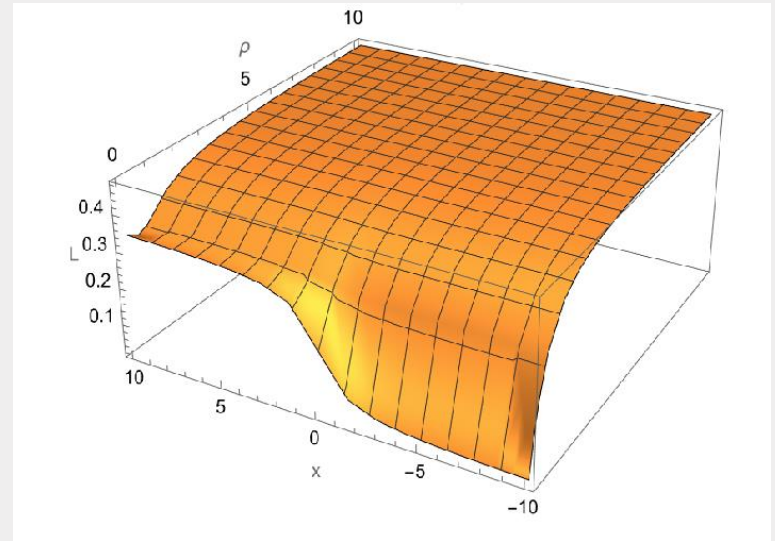


## II. Bubble Walls

### Dynamics of Bubble Wall

Ansatz of initial condition is chosen as

$$L_0(\rho, x) = \frac{1}{2} \left( 1 - \frac{2}{\pi} \text{Arctan}(x) \right) L_1(\rho, x) + \frac{1}{2} \left( 1 + \frac{2}{\pi} \text{Arctan}(x) \right) L_2(\rho, x)$$



□  $L_1$  and  $L_2$  are the  $x$  independent solutions for the true vacuum and metastable vacuum. They are explicit solutions of the equations of motion as described in the phase transition section.

□ The Arctan functions simply transition us from one solution to the other as we move in  $x$  around  $x = 0$

□  $L_1$  and  $L_2$  are the  $x$  independent solutions for the true vacuum and metastable vacuum. They are explicit solutions of the equations of motion as described in the phase transition section.

# II. Bubble Walls

## Dynamics of bubble wall

Other Boundary Conditions

$$\partial_t L[\rho, 0, x] = 0$$



$$L[\rho, t, -x_{\max}] = L_0[\rho, -x_{\max}]$$



$$L[\rho, t, x_{\max}] = L_0[\rho, x_{\max}],$$



$$L[\rho_{UV}, t, x] = L_0[\rho_{UV}, x]$$

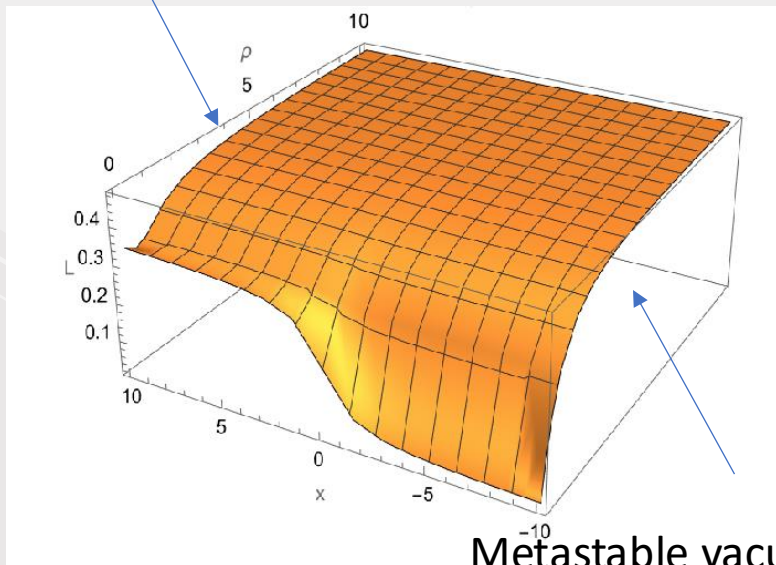


$$\partial_\rho L[0, t, x] = 0$$



- Static initial configuration
- left and right configuration remain in the vacuum and metastable vacuum configurations
- Solution  $L(\rho, t, x)$  with the same UV mass at any time
- IR regularity condition for Minkowski embeddings

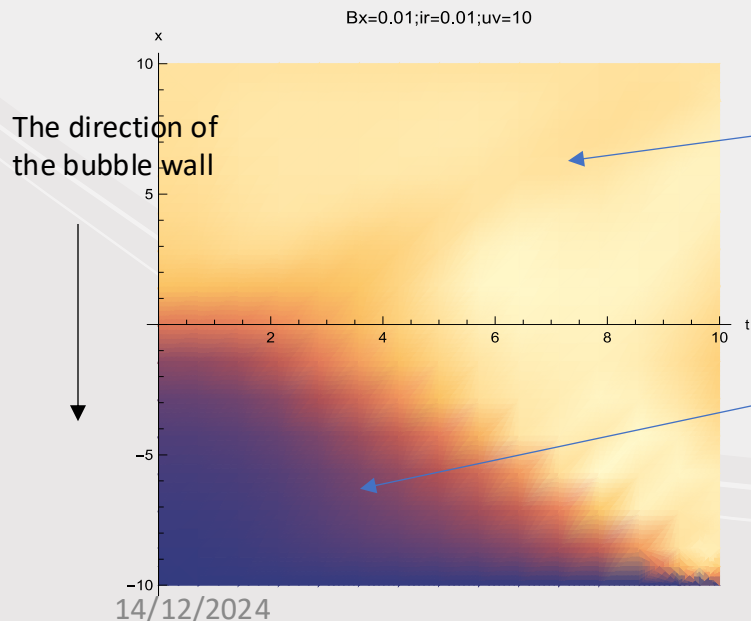
True Vacuum



## II Bubble Walls

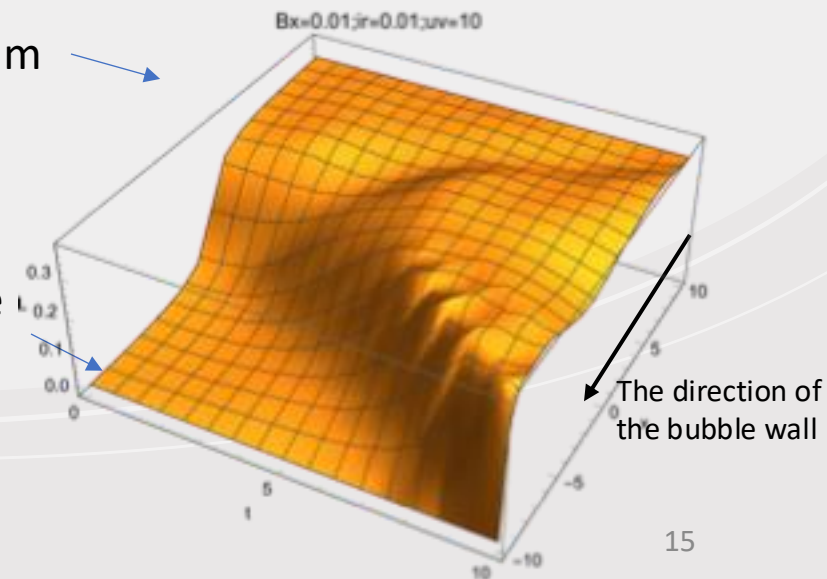
### The evolution of the **embeddings** and pressures

- ❑ The below are the plots of  $L(0)$  as a function of time and  $x$ .
- ❑ The metastable vacuum is on the left and the true vacuum on the right on the right graph.
- ❑ The bubble wall moves from right to left on the right graph.
- ❑ Since the embedding,  $L(\rho, t, x)$ , also depends on the holographic coordinates  $\rho$ , waves can also propagate along the configuration in  $\rho$ , but we cannot show this additional dimension configuration on the paper.



True vacuum

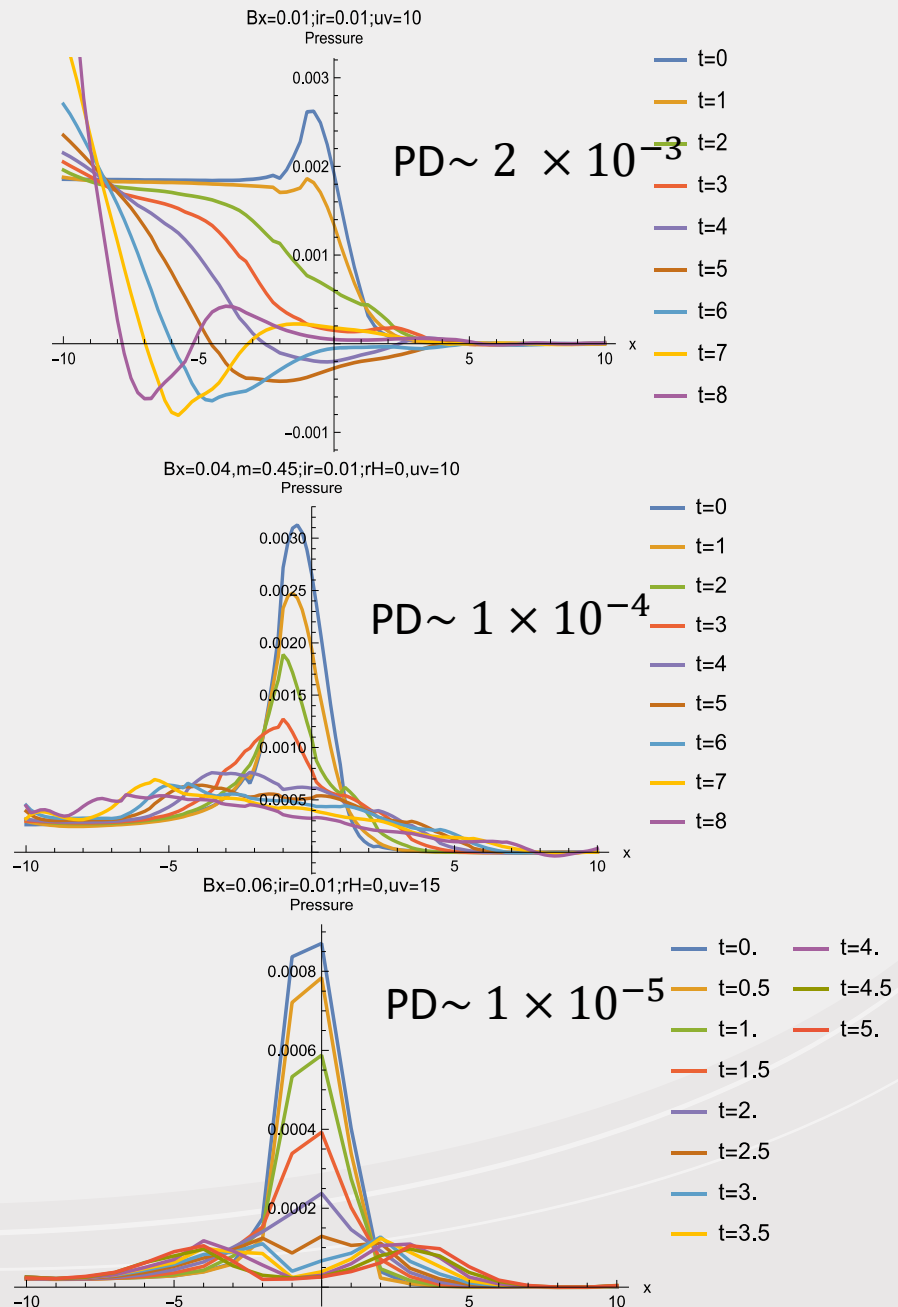
Metastable vacuum



## II Bubble Walls

### The evolution of the embeddings and pressures

- ❑ As a solution, the action integrated along  $\rho$  to give the local energy density (or pressure) which is plotted on the right.
- ❑ The wall's speed in the absence of friction has quickly approached the speed of light  $c = 1$ .
- ❑ As we decrease the pressure difference, the bubble wall slumps instead of moving.



## II Bubble Walls

### Bubble Walls at Finite temperature – The method

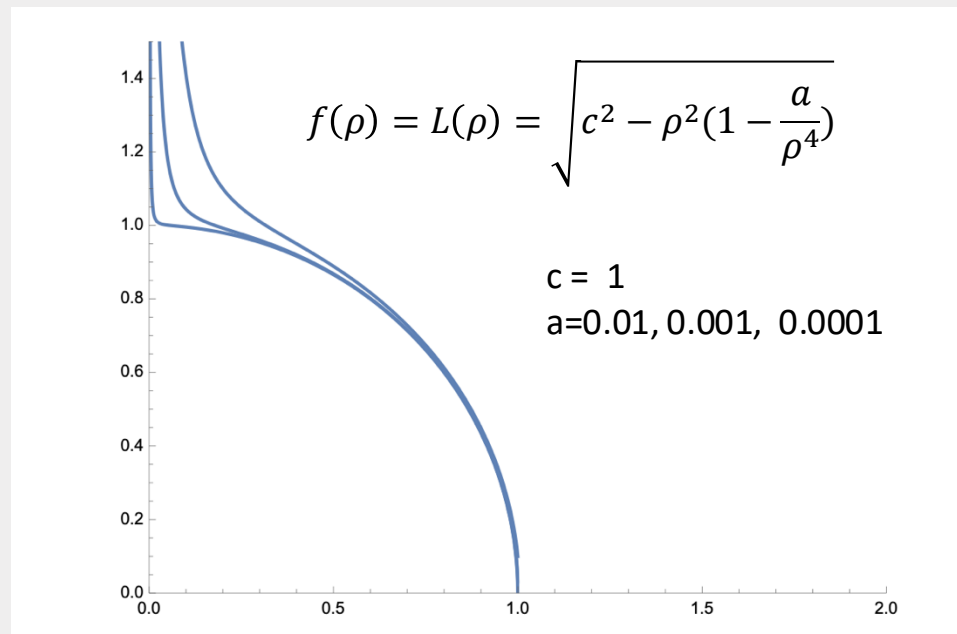
- ❑ To study the effect of a thermal bath on the bubble wall motion we will include non-zero black hole radius  $r_H$ .
- ❑ We interpolate the BH embeddings and the MK embeddings by turning the space in the  $L - \rho$  plane outside the black hole into a square coordinate grid.
- ❑ To get the square space, we use the new coordinate

$$\tilde{L} = L;$$

$$\tilde{\rho} = \rho - \frac{\sqrt{c^2 - L^2 + \sqrt{4a + (c^2 - L^2)^2}}}{\sqrt{2}}$$

- ❑ In principle, we calculate the DBI action of D7 brane in this tilde coordinate system:

$$\mathcal{L} = (f(\tilde{L}) + \tilde{\rho})^3 \tilde{g} \tilde{h} \sqrt{(\tilde{L}' f'(\tilde{L}) + 1)^2 + \tilde{L}'^2} \\ \times \sqrt{1 + \frac{b^2 \tilde{L}^2}{\tilde{h}((f(\tilde{L}) + \tilde{\rho})^2 + \tilde{L}^2)^2} + \frac{Bx^2}{\tilde{h}^2((f(\tilde{L}) + \tilde{\rho})^2 + \tilde{L}^2)^2}}$$



Parameter  $c$  is related to the BH radius and  $a$  plays the role of a cutoff away from the horizon

## II Bubble Walls

### Bubble Walls at Finite temperature – Boundary Conditions

$$L[\rho, 0, x] = L_0[\rho, x]$$

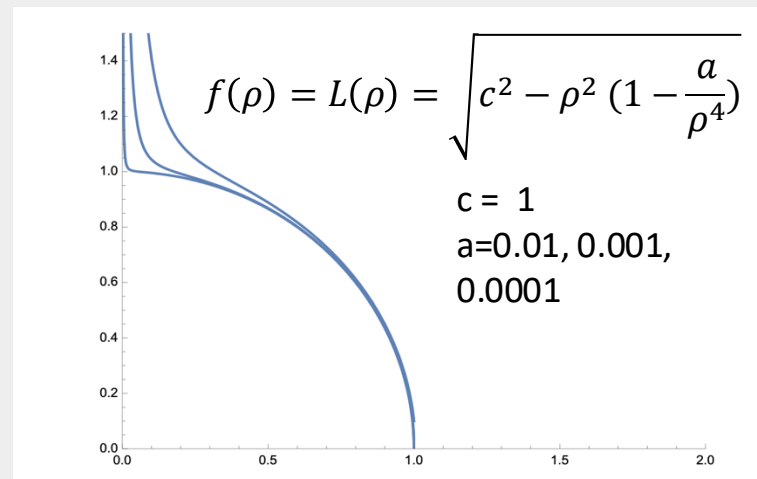
$$\partial_t L[\rho, 0, x] = 0$$

$$L[\rho, t, -x_{\max}] = L_0[\rho, -x_{\max}]$$

$$L[\rho, t, x_{\max}] = L_0[\rho, x_{\max}],$$

$$L[\rho_{UV}, t, x] = L_0[\rho_{UV}, x]$$

$$\partial_\rho L[0, t, x] = 0$$



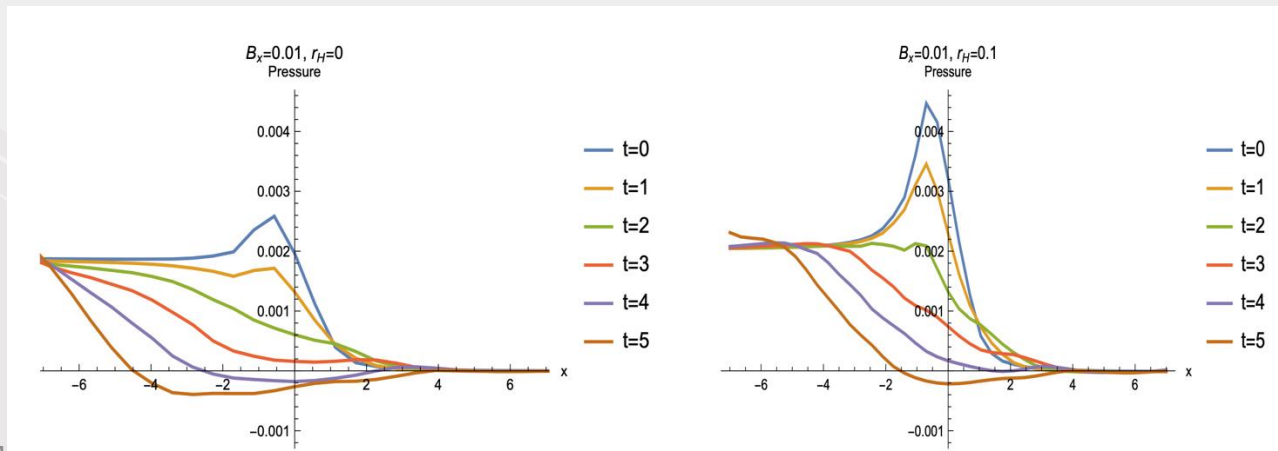
- ❑ We use the same boundary conditions as those at zero temperature. (i.e. relabelling  $L \rightarrow \tilde{L}, \rho \rightarrow \tilde{\rho}$ )
- ❑ For the Minkowski region, we pick  $\tilde{L}'(\tilde{\rho})=0$ .
- ❑ For the black hole region, we pick the same condition  $\tilde{L}'(\tilde{\rho})=0$ . Since near the black hole horizon, the solutions have an attractor behavior and very insensitive to the boundary condition choice.

## II Bubble Walls

### Bubble Walls at Finite temperature – The result I

We can now present two example simulations that display the behaviours we observe with temperature.

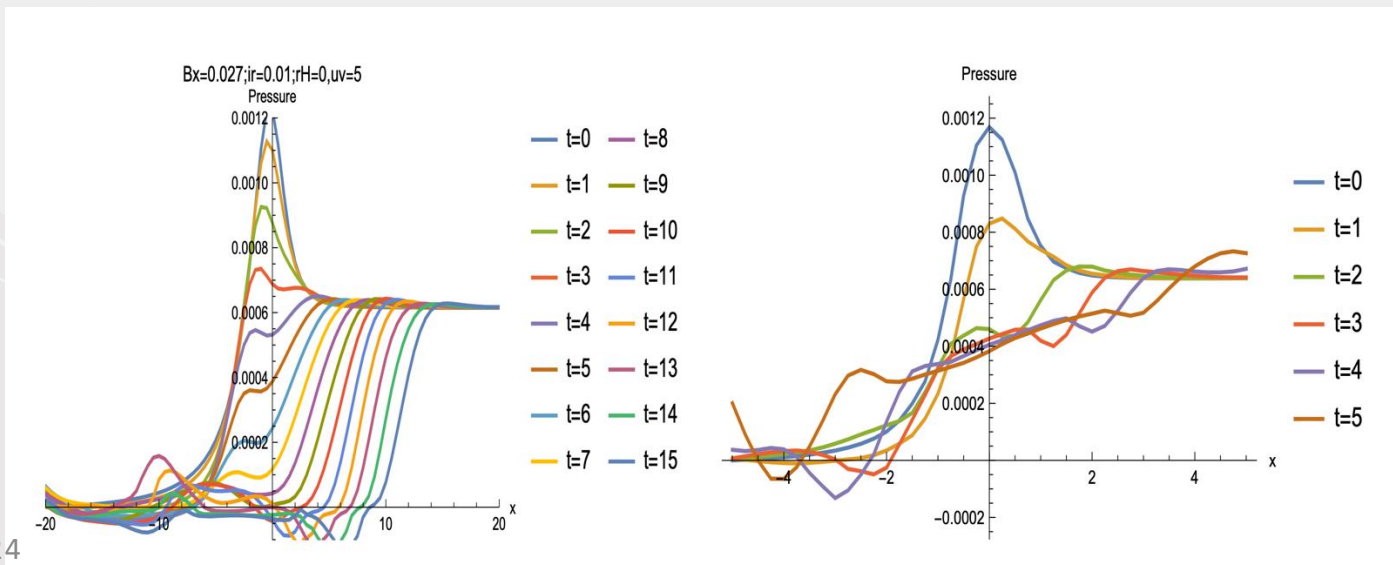
- ❑ As shown on the left, the configuration at zero temperature was a clear cut wall that accelerated quickly to move at  $c$ .
- ❑ To compare, the right shows that the speed of the wall, at least in the initial phase of acceleration, is slowed to  $0.7c$  showing the presence of friction from the thermal bath.
- ❑ Note the pressure plots are not identical at  $t = 0$  with the thermal configuration having more energy stored in the wall - it is possible to adjust this by adding a further parameter writing  $\text{ArcTan}(\gamma x)$  in our initial ansatz and varying  $\gamma$ . The conclusion does not change as to the behaviour though when we run those simulations



## II Bubble Walls

### Bubble Walls at Finite temperature – The result II

- ❑ On the left, we look at a configuration with lower pressure difference. At  $T = 0$ , the evolution goes through an initial slump before developing into a moving domain wall.
- ❑ On the right, it is a configuration with the same pressure difference but evolved at finite  $T = 0.2$ .
- ❑ The early stages show a possible new behaviour distinct from simply an accelerating wall.
- ❑ Here the configuration shows two pressure waves moving in opposite directions with a pressure plateau between them.
- ❑ The figure shown is the most controlled example we have seen of this behaviour. It would be interesting to fully explore the parameter space in the future to see how these walls evolve at different parameter choices. For the moment this is beyond the Mathematica analysis we present here.



# Summary

- ❑ We showed that the D3/D7 probe brane with a background  $B$  field and an axial gauge field  $b$  has a first order phase transition, and a critical point in the B-M plane.
- ❑ The properties of the first order transition and critical point allow us to dial the parameters (pressure difference and barrier height) of the bubble walls. (We show the zero mode at the critical point.)
- ❑ It is shown that bubble wall interpolated by the metastable vacuum and the true vacuum in the spatial coordinates reach the speed of light in the absence of friction for large pressure difference.
- ❑ The bubble wall stops moving as the pressure difference is small.
- ❑ We have also developed methods to allow us to add in a thermal bath. The resulting simulations showed new behaviours beyond the zero temperature results including slowing friction and a double wall structure in cases with smaller pressure differences.

## Future work

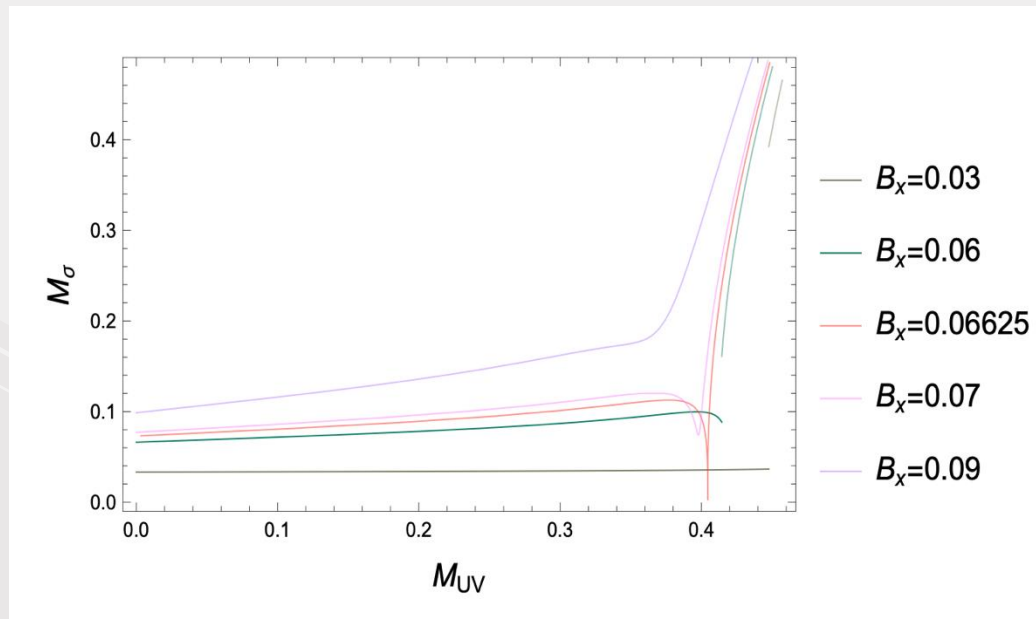
- ❑ Our results with a thermal bath here have been preliminary because we have allowed ourselves to depend on the MATHEMATICA NDSolve black box which in the future we hope to improve upon. Hence, the priority is to optimize the code to solve PDEs. or transfer the code into a more efficient language, such as Julia.
- ❑ It would be interesting to fully explore the **parameter space** in the future to see how these walls evolve at different parameter choices. For the moment this is beyond the Mathematica analysis we present here.
- ❑ Finally, we hope this study will inspire further investigations into bubble walls in other holographic settings, such as top-down or bottom-up models for QCD, to better understand how generic the behaviors we observe are in strongly coupled systems. If gravitational wave signatures of a phase transition in the early universe are observed in experiments, having these descriptions of strongly coupled cases could become particularly significant and interesting.

Thank you!

# Back up slides

## Zero mode at critical point

- ❑ We scan the meson spectrum along the first order phase transition with critical end point, and there is a massless modes near the critical point
- ❑ The critical point should correspond to the values of parameters where the free energy between the two competing vacuum states become degenerate and the barrier between those vacua falls to zero height.
- ❑ The Higgs/sigma mode of the symmetry breaking should therefore see a flat direction in the potential at this point and there should be a massless state in the spectrum.



# Back up slides

## Phase diagram at finite temperature

- The first order phase line in the theory with  $b = 1$  in the  $M_{UV} - B_x$  plane at zero temperature on the left. On the right the thermal phase transition (BH-Mink) at different temperatures.
- The Weyl semi-metal phase where the D7 embeddings end at  $\rho = L = 0$  will immediately become a solution that ends on the black hole horizon (this phase has melted quasi-normal mode states rather than stable mesons )

Carlos Hoyos, Karl Landsteiner .etc : 0612169

